SYNTHESIS AND MAGNETIC PROPERTIES OF NANOSIZED SILVER-IRON COMPOSITE NANOPARTICLES

Ke Liu[1], Shengchun Yang[1], Xiaohui Ma[2], Zhimao Yang[1]
1. Non-equilibrium Condensed Matter and Quantum Engineering Laboratory, the Key Laboratory of Ministry of Education, Xi'an Jiaotong University, Shaan Xi, 710049, P.R.China
2. Beijing GaoGuoKe Technology Co., Ltd., Beijing, 100044, P.R.China

1. Introduction

Combining two or more components into a single nanoparticle has been considered to be a facilitated method to tailor their physical and chemical properties by changing their charge density, functionality and crystalline structure[1-3], create multi-functional composite nanoparticles[4,5] and even generate novel bulk materials[6]. Therefore, these kinds of compound nanoparticles have attracted considerable attention in recent years.

Composite nanoparticles consisting of nonferromagnetic silver and ferromagnetic iron metals are of interest because they are easy to be functionalized and the chemically active iron atoms can be well protected from being oxidized. Additionally, due to the different Fermi energies of silver and iron, a space-charge region at Ag/Fe interphase boundaries may enhance the solid solubility of both components and change the state of emission of electrons[7]. Therefore, the nanocomposites combing silver and iron metals may have great potential application in magnetic, electric, catalytic and biochemical fields.

Many methods have been developed to synthesize the metal composite nanoparticles. Ban et al. obtained Au-Co nanoparticles by a homogeneous non-aqueous solution reactions method[8], Lin et al. synthesized gold-coated iron (Fe@Au) nanoparticles by using a unique reverse micelle method[9], Shouheng Sun et al. prepared FePt nanoparticles by reduction of platinum acetylacetonate and decomposition of iron pentacarbonyl in the presence of stabilizers[10]. However, only few synthetic procedures were developed to prepare the ferromagnetic AgFe composite nanoparticles. Chinmay Damle et al. developed a method by the in situ reduction of the metal ions to get nanoscaled AgFe composite within thermally evaporated fatty acid films.

In the present work, the synthesis of such composite nanoparticles in reverse micelles followed by a direct coating method in DMF was performed. The results showed that that as-synthesized composite nanoparticles, consisting of α-iron and FCC silver, exhibit excellent magnetic properties.

2. Experimental

The reverse micelles method was used to prepare the silver coating iron nanoparticles. And the microemulsion was formed by using cetytrimethylammonium bromide (CTAB) as the surfactant and the 1-butanol as cosurfactant, octane as the oil phase and aqueous reactants as the water phase. The molar ratio of water to CTAB was selected to be 10:1 to control the size of the nanoparticles. In a typical procedure, the reverse micelles were formed by dissolving 10 g CTAB and 5 mL aqueous solution containing certain amount of metal irons and reductant into an organic mixture of 40 mL octane and 12 mL 1-butanol. Firstly, two batches of reverse micelles solution containing 1.0 g $FeCl_2 \cdot 4H_2O$ and 0.38 g $NaBH_4$, respectively, were sonicated at Ar atmosphere, until the solutions became clear. Then they were mixed together under vigorous stirring and the mixture immediately turned into black. It indicated that the iron nanoparticles were formed. The stirring was continued at room temperature for 30 min. The dark powder of iron nanoparticles was separated with a magnet and washed with C_2H_5OH several times at Ar atmosphere to remove the surfactants, Br^- and Cl^- ions. The iron nanoparticles were stored at Ar atmosphere.

To prepare the 10 % (wt%) iron doped silver composite nanoparticles, the iron nanoparticles were dispersed in 70 mL anhydrous DMF through mechanically stirring for 10 min. 0.46 g $NaBH_4$ and 4.0 g $AgNO_3$ were dissolved into 10 ml DMF, separately. After $NaBH_4$ solution was added into the suspension of iron nanoparticles, $AgNO_3$ solution was dropped into this intermixture. After stirred for 1h at Ar atmosphere, the final powder with 10% iron (wt%) was separated with the magnet field and washed with ethanol several times to remove the remained surfactants. The sample was dried in vacuum. In experiment, other two samples with different Fe mass fraction (5 % and 25 %) were synthesized by using the same method.

The crystal structure of the products was measured with the Rigaku D/MAX-2400 Powder X-ray diffractometer. The morphology and elemental analysis of composite nanoparticles were performed by using a JSM 7000F SEM and a JEM-1200EX TEM. Samples for TEM measurements were prepared by dropping colloidal solutions of AgFe nanocrystals in ethanol on carbon coated copper-grid. Magnetic measurements were performed using a VSM-LakeShore7307. Approximately 20 mg of samples right after the synthesis was placed in the platform to get the magnetic property.

In order to investigated the anti-oxidation properties of as synthesized AgFe composite nanoparticles, the sample with 10 % iron (wt %) was heated at 573 K, 673 K, 773 K in air for 1 h, respectively, and samples with 5 % and 25 % iron (wt %) were heated to 673 K in air for 1 h. The crystal structure of the heated products was measured by using X-ray diffractometer.

3. Results and discussion

The XRD patterns of three samples confirm that the peaks are corresponding to the FCC metallic silver diffraction, as shown in Figure 1. The diffraction peaks of α-iron overlapping some ones of silver, (200), (220), (222), illuminates the pattern of the α-iron is hidden in the pattern of silver. The size of nanoparticles can be calculated from diffraction peaks with stronger intensity, (111), (200), (220), using the Scherrer equation[10]. The size is 30.8, 24.6, 19.2 nm corresponding to iron mass fractions of 5 %, 10 % and 25 %, respectively, as shown in Figure 1. It suggests that the composite particle size decreases slightly with the increase of iron ratios. This could be attributed to the reason as follow: the size of iron nanoparticles should be the same for all samples due to the same method and condition of synthesizing iron nanoparticles. The thickness of silver crystal on the surface of iron nanoparticles decreases with decreasing of silver ratios. In the end, the size of composite nanoparticles, consisting of the iron particle size and the silver crystal thickness, decreases with the increase of iron ratios.

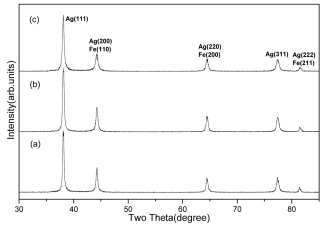

Figure 1. XRD patterns of samples with (a) 5 % Fe, (b) 10 % Fe and (c) 25 % Fe in weight.

SEM images of the samples with three different content of iron are presented in Figure 2 (a), (b) and (c). The size of particles seems to be almost 100 nm. The reason is that the particles, which are still magnetic at the room temperature, aggregated in the grids. It is found that the particles size decreased as the concentration of iron increased. Furthermore, due to the magnetic particles interact with the electron beam; the image is more blurred as the concentration of iron increases.

The energy-dispersive X-ray spectrum of the samples roughly indicates that the content of iron and silver is 5.92 % and 94.08 % for sample in Figure 2(a), 10.84 % and 89.16 % for sample in Figure 2(b), 24.46 % and 75.54 % for sample in Figure 2(c). This is in good agreement with the designed ratio of composition, illustrating that the loss of iron is almost neglectable in the process of particles synthesis.

Figure 3(a) shows TEM image of Ag-Fe composite nanoparticles with 10 % iron. From TEM image, the size distribution of the composite nanoparticles was measured to be 19.8 nm, consistent with the results of XRD analysis. But this is much smaller than the results from SEM image, which can be attributed to the aggregation of the nanoparticles. The dark iron center and gray silver surface of particles are visible. Figure 3(b) is the corresponding electron diffraction, by use the Miller-Bravais indices (hki) to the particles, from inner to outer, SAED ring patterns correspond to indices (111), (200), (220), (311) of silver, and (110), (200) of iron.

The magnetic response of the composite nanoparticles can be easily detected by using a magnet. Figure 4(a) shows the as-synthesis nanosized silver-iron composite nanoparticles with 10 % iron dispersed in water. When a magnet was near the dispersion, the nanoparticles began to move and aggregate on the flask wall (Figure 4(b)). The time for such process is around 30 min in this magnetic field.

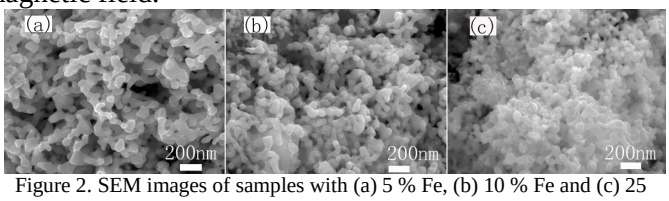

Figure 2. SEM images of samples with (a) 5 % Fe, (b) 10 % Fe and (c) 25 % Fe.

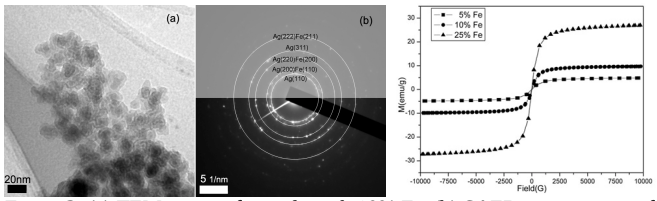

Figure 3. (a) TEM image of sample with 10% Fe, (b) SAED ring patterns of the region of (a), (c) the magnetic hysteresis loops of the samples with iron ratios of 5 %, 10 % and 25 %,at 300K.

Magnetic hysteresis loops of as-synthesized powder samples at 300 K are shown in Figure 3c, no significant hysteresis phenomenon was observed. All of the three samples display superparamagnetic property. Saturation magnetization (M_S) of these samples is 6.0, 9.7 and 27.0 emu/g, corresponding to the samples with iron ratios of 5 %, 10 % and 25 %, respectively.

4. Conclusions

In summary, the nanosized silver-iron composite nanoparticles were synthesized by two steps method in reverse micelles and DMF. The result of XRD, SEM and TEM measurement illustrated that α-iron survives in composite nanoparticles. The size of particles decreases from 30.2 to 19.8 nm with the decrease content of Fe. The XRD patterns of the heated particles dedicated that these composite nanoparticles have well anti-oxidation properties compared to pure Fe particles even at high temperature (773K). And the magnetic saturation of the superparamagnetic particles can increase to 27 emu/g when the content of Fe was 25 % with the protecting of silver.

Reference

[1] Stamenkovic V. R., Fowler B., Mun B. S., etal, Science 315 (2007) 493-497.
[2] Caruso B. F., Advanced Mater. 13 (2001)11-22.
[3] Lee C.-C., Nanotechnology 17 (2006) 3094-3099.
[4] Cho S-J, Kauzlaricha S. M., Olamit J., etal, J. App. Phys. 95 (2004) 6804-6806
[5] Gao T., Li Q., Wang T., Chem. Mater. 17 (2005) 887-892.
[6] Sun S., Murray C. B., Weller D., etal, Science 287 (2000) 1989-1992.
[7] Gleiter H., Weissmüller J., Wollersheim O., Wurschum R., Acta materialia 49 (2001) 737-745.
[8] Ban Z. H., O'Connor C. J., Processing, Characterization and Theory 818 (2004) 113-116.
[9] Lin J., Zhou W., Kumbhar A., etal, J. Solid State Chem. 159 (2001) 26-31.
[10] Damle C., Biswas K., Sastry M., Nanotechnology 13 (2002) 103-107.
[11] Joel A. Haber, William E. Buhro, J. Am. Chem. Soc. 120 (1998) 10847-10855.